ORIGINAL ARTICLE

ANATOMIA HISTOLOGIA EMBRYOLOGIA
JOURNAL OF VETERINARY MEDICINE

WILEY

Anatomy, Morphometry and Radiography in the thoracic limb bones of the Patagonian Huemul Deer (*Hippocamelus bisulcus*)

Paulo Salinas[1] | Samuel Núñez-Cook[1] | Abigail Arenas-Caro[1] | Luis Moreno[2] |
Escarlet Curihuentro[2,3] | Fernando Vidal[3,4,5,6]

[1]Institute of Biology, Faculty of Sciences, Pontificia Universidad Católica de Valparaíso, Valparaíso, Chile

[2]School of Veterinary Medicine, Universidad Santo Tomás, Temuco, Chile

[3]Fauna Andina, Wildlife Conservation and Management Center, Villarrica, Chile

[4]Unit of Wildlife Conservation and Management, Universidad Santo Tomás, Temuco, Chile

[5]IUCN, Deer Specialist Group, Apple Valley, MN, USA

[6]Fundación Huilo Huilo, Wildlife Department, Neltume, Panguipulli, Chile

Correspondence
Paulo Salinas, Animal & Experimental Morphology Lab, Institute of Biology, Faculty of Sciences, Pontificia Universidad Católica de Valparaíso. Av.Universidad # 330, Curauma 3100000 Valparaíso, Chile.
Email: paulo.salinas@pucv.cl

Abstract

The aim of this study was to provide morphometric, anatomic and radiographic data of the thoracic limb bones of the Patagonian Huemul (*Hippocamelus bisulcus*) including a functional interpretation of this, as a reference for clinical use, biomedical research and teaching purposes. Currently, the Patagonian huemul deer is in danger of becoming extinct due to multiple causes. Research carried out for its conservation has focused mainly on its ecology and pathology, leaving gaps in biological knowledge, which is basic and important for its comprehension. This study was conducted to reveal the gross osteology and radiology features of the thoracic limb bones of the Patagonian huemul deer. The osteological findings suggest the presence of powerful flexor muscles in the scapulohumeral and elbow joints, useful to cushion the jumps. Also, the principal nutrient foramen of Patagonian huemul differs in position with respect to domestic ungulates, which may be important to consider during surgical procedures. Finally, the radiographic data can provide new information about the tissue loading conditions in Patagonian huemul, so that this new knowledge can be of great importance for a better understanding of mechanically induced or adaptive changes in bone produced by habitat or other ecological phenomena.

KEYWORDS
anatomy, deer, huemul, osteology, skeleton, wildlife

1 | INTRODUCTION

The Patagonian huemul (*Hippocamelus bisulcus* Molina, 1782) is a medium-sized deer with characteristic bifurcated antlers only in males, a withers height of one metre from the ground, a length of 118–163 cm and a variable weight around 40–100 kg. Females, on the other hand, are slightly smaller and thinner and do not present antlers. The huemul is endemic of the Andes region of Chile and Argentina and was originally distributed in an extension from 34°–54°S in the southern cone. Now, however, they are not observed from 34°–41°S, in neither of the two countries. Its global population varies between 1,500 and 2,000 individuals in Chile and 300 and 600 in Argentina, with an estimated

size reduction of 99% and a habitat loss of 50% (Iriarte, Donoso, Segura, & Tirado, 2017; Vila, López, Pastore, & Serret, 2006). The species is internationally declared endangered, with fragmented populations and decreasing number of individuals due to anthropogenic causes, such as human settlements and agriculture, limiting accessibility to the valleys and eliminating seasonal migration (Black-Decima et al., 2016). However, the greatest impact on the population decline has been caused by infectious diseases transmitted by domestic livestock, such as parapoxvirus (Vila et al., 2019), caseous lymphadenitis (*Corynebacterium pseudotuberculosis*, Morales et al., 2017), bovine paratuberculosis (*Mycobacterium avium*; Salgado et al., 2017), bovine viral diarrhoea (bovine viral diarrhoea virus; Corti, Saucedo, & Herrera, 2013) and sheep scab

(*Psoroptes ovis*; González-Acuña, Saucedo, Corti, Casanueva, & Ciccino, 2009).

Current conservation strategies consider the creation of protected areas, ex situ conservation projects and captive breeding for reintroduction, but these have not been sufficient, with the population presenting almost no recovery. Nutritional ecology has been proposed as the most parsimonious explanation to this situation, especially due to the deficiencies of selenium and iodine that negatively affect bone metabolism and consequently the appendicular and axial skeleton. Moreover, disruption of normal migration and inaccessibility to fertile lands (Flueck, 2015) could explain the high prevalence of skeletal injuries and diseases in Chile (87%) and Argentina (57%). The main skeletal injuries and diseases reported were osteomyelitis, osteoarthritis, periodontitis, hoof injuries and exfoliation of incisors. These records argue the need to propose new research approaches with the purpose of understanding the aetiology of osteopathies and of closing gaps regarding their biology (Flueck & Smith-Flueck, 2017).

Knowledge about the Patagonian huemul anatomy is scarce, focusing mainly on the comparison—perhaps erroneous—of biometric measurements of its limbs with high mountain animals such as: *Capra ibex*, *Rupicapra rupicapra*, *Ovis canadiensis*, *Oreamnos americanus* (Flueck & Smith-Flueck, 2011), without emphasising macro- or microscopic anatomy. In this regard, the generation of new knowledge is highly relevant, essentially in relation to the structure and function (Vélez-García, Monroy-Cendales, & Castañeda-Herrera, 2018), given its usefulness in fieldwork research with interpretive and teaching purposes. Surgery, pharmacology and especially anaesthesiology have made significant progress in the field of veterinary medicine of wild animals; however, this progress has not kept pace with the generation of new anatomical knowledge of the Patagonian huemul. The aim of this study was to provide morphometric, anatomic and radiographic data of the bones of the thoracic limb of the Patagonian Huemul (*Hippocamelus bisulcus*) including a functional interpretation of this, as a reference for clinical use, biomedical research and teaching purposes.

2 | MATERIALS AND METHODS

2.1 | Specimens

Three skeletons of Patagonian huemul deer (*Hippocamelus bisulcus*) were used, which were denominated as: "specimen-A," male specimen, deceased for causes not related to this research, obtained by exhumation one year prior to the study (Source: Fauna Andina, Pedregoso sector, Villarrica (39°16'00"S, 72°13'00"W) in La Araucanía Region, Chile; 227 m.a.s.l., collected on October 20, 2014) within the Resolution framework No. 1,490 (December 22, 2003) of the Agricultural and Livestock Service of Chile (SAG), "specimen-B" and "specimen-C" belonged to the collection of the Chilean National Museum of Natural History (NMNH), both of unknown sex ("B": NMNH N°1947; source: Villa Cerro Castillo, Aysen, in General

Carlos Ibáñez del Campo Region, 46°07'15.0"S, 72°09'20.0"W, 404 m.a.s.l., collected on January 3, 2005; and "C": NMNH/MAM N°1948, Chilean origin, no background).

2.2 | Gross anatomy, morphometry and radiography

A descriptive and morphometric study of the appendicular skeleton of the three huemul was performed from simple visual observation, with calipers and a flexible tape measure. To avoid observer bias, the bones were described and measured by three independent evaluators. In long bones, we measured the following: total length, narrowest width of diaphysis and greater width of epiphysis. In flat bones, length margins were measured, among other metrics variables specific to each bone. The obtained data (mean ± *SD*) were sorted in Excel tables (Microsoft Office Professional Plus 2013, Windows 7 Professional 2009). The terminology used in this study is that of *Nomina Anatomica Veterinaria* 6th Edition (Revised) (ICVGAN, 2017). The radiographic study was used to describe the opacity and density of the compact and trabecular bone tissue. The radiographic findings were correlated with the bone samples. The images were obtained by indirect digital radiology. An ORANGE 9020 HF X-ray generator (EcoRay Co., LTD., Seoul, Korea) was used, with a configuration of 60 Kv and 2.5 mAs, at a distance of 100 cm. Radiographic carbon fibre chassis with phosphor panel of 24 × 30 cm was used. The digitalisation of the images was carried out through the portable veterinary radiography (CR) system (iCRcoTM, iCR Chrome Vet model, USA). The images were obtained using DICOM XCTM software using a Dell Inspiron 15 7000 Series PC with CORE i7 processor. The radiographic findings were correlated with the bone samples.

3 | RESULTS

The thoracic limb bones were represented by the scapula, humerus, radius, ulna, carpal and hand bones. No coracoid process or clavicle was observed. The stylopodium was represented by the humerus (*skeleton brachii*). The zeugopodium was represented by the radius and the ulna (*skeleton antebrachii*). The autopodium (*skeleton manus*) presented three subsegments: carpal, metacarpus and digits. The measurements of bones of the thoracic limb are described in Table 1.

The scapula was flat and triangular (Figure 1). The costal surface presented a concavity flanked by the cranial and caudal borders. The facies serrata was observed, and a broad concave subscapular fossa, in which define lines of muscular insertion were distinguished. The lateral surface presented a large spine of the scapula, which divided the supraspinous fossa (cranial) from the infraspinous fossa (caudal). In addition, the surface of both fossae was smooth and slightly concave, occupying one third and two third of the lateral surface of the scapula, respectively. The sharp and pointed acromion was present in the most distal part of the spine of the scapula. In the cranial border, a convex proximal half and a concave distal half were observed, the latter being part of the scapular notch. The distal quarter

TABLE 1 Morphometry of the thoracic limb bones of the Patagonian Huemul Deer (mean ± SD)

|	Length (mm)	
	Right n = 3	Left n = 3
Scapula		
Cranial border	207.53 ± 16.31	212.65 ± 3.61
Dorsal border	126.48 ± 6.00	121.70 ± 3.39
Caudal border	194.50 ± 13.46	200.20 ± 0.71
Width of glenoid cavity	46.37 ± 2.22	44.38 ± 1.00
Maximum scapular height	47.45 ± 3.76	45.31 ± 4.64
Humerus		
Total	229.87 ± 20.10	227.17 ± 24.49
Width of proximal epiphysis	65.49 ± 3.71	65.62 ± 6.06
Width of diaphysis	20.41 ± 1.24	19.55 ± 0.54
Width of distal epiphysis	48.31 ± 3.61	46.71 ± 2.59
Radius		
Total	199.60 ± 11.67	194.18 ± 3.49
Width of proximal epiphysis	40.82 ± 3.21	37.53 ± 1.38
Width of diaphysis	23.83 ± 0.72	20.64 ± 2.31
Width of distal epiphysis	40.32 ± 2.43	38.03 ± 0.04
Ulna		
Total	257.04 ± 36.93	295.82[a]
Width of proximal epiphysis	39.10 ± 1.84	38.29 ± 1.65
Width of diaphysis	1.66 ± 0.15	1.73 ± 0.03
Width of distal epiphysis	13.00 ± 0.01	13.04[a]
Metacarpals		
Total	162.77 ± 3.16	159.13[a]
Width of proximal epiphysis	34.48 ± 1.60	33.45[a]
Width of diaphysis	19.38 ± 1.64	18.16[a]
Width of distal epiphysis	37.61 ± 4.96	33.45[a]

[a]n = 2.

presented a slight concavity. The ventral angle was articulated and corresponds to the glenoid cavity. The scapular neck was narrow and had lines of muscular insertion in its latero-caudal portion. Moreover, it had three bony accidents: (a) the glenoid cavity, circumscribed by the well-defined glenoid notch and oriented laterally, (b) the supraglenoid tubercle, located cranially and laterally and (c) the coracoid process, pointed and with a hook-like shape towards the medial. The principal nutrient foramen (FNP, foramen nutrition principles) was present in the latero-caudal aspect of the scapular neck and in the distal end of the infraspinous fossa. Radiolucent zones were observed in the region of the supra and infraspinous fossa. Radiopacity was observed in the spine of the scapula and especially in the subchondral cortical plate of the articular eminence. In addition, a large amount of trabecular bone tissue was observed in the region of the ventral angle.

The humerus was long and prominent (Figure 2). The proximal epiphysis presented three eminences: (a) a greater tubercle (*tuberculum majus*) of lateral location, shaped like a laterally rough and

convex oval cap similar to a three-sided prismatic peak: a slightly rough cranial surface, a concave medial surface (lateral slope of the intertubercular groove) and one lateral surface larger than the others, which presented a rough surface, (b) the minor tubercle (*tuberculum minus*), of medial location and three surfaces: lateral (concave, lateral side of the intertubercular groove), cranial (rough and well defined) and medial (smooth and well defined) and (c) the head of the humerus, of caudal location accompanied of the humeral neck. The diaphysis was cylindrical and had a helical sulcus (*sulcus m. brachialis*) of ventromedial obliquity. The rotation of the diaphysis generated two margins. The cranial margin (humeral crest) had a deltoid tuberosity in its proximal third. In addition, a line of the triceps muscle that extended to teres minor tuberosity (*tuberositas teres minor*) was observed. The caudal margin was represented by the lateral supracondylar crest, which was observed as the dorso-medial projection of the lateral epicondyle. The teres major tuberosity (*tuberositas teres major*) was observed in the medial surface of the diaphysis, around it, there was a small rough area of muscular insertion. The FNP was located proximal to the lateral supracondylar ridge. The diaphyseal section was just between the middle and distal third of the diaphysis. The distal epiphysis was small and presented bony eminences: the humeral condyle, of cranial location, formed by a small (lateral) *capitulum*, and the trochlea (medial); and two non-articulate caudal epicondyles: lateral and medial, the latter being the most prominent. Both epicondyles flanked a deep olecranon fossa (*fossa olecrani*). Proximal to the condyle was the radial fossa (*fossa radialis*), of moderate depth. Areas of trabecular radiolucent bone tissue were observed in epiphysis proximal and distal. In addition, radiopaque compact bone tissue was observed in the diaphysis and on the surface of the greater and minor tubercle.

The radius (*radius*) was long (Figure 3). It presented a longitudinal curvature with a longitudinal caudal concavity. In the proximal epiphysis, in the radial head (*caput*), a wide articular fovea (*fovea capitis radii*) was observed. Tuberosities of ligament attachment were located on both sides of the joint cavity. On the caudal surface of the caput, a bony border was observed, whose structure resembled a belt with which the radio articulated with the ulna (*circumferentia articularis*). The radial tuberosity was observed at cranio-medial location, adjacent to the medial surface of the radial neck. The diaphysis presented a cranial smooth surface and a caudal rough surface, well-defined lateral and medial margins, also an oval and widened cross-sectional area towards distal. The cranial surface of the diaphysis was smooth and convex. The caudal surface, on the contrary, was rough and concave, presenting a rough line in its distal two thirds, suggesting the presence of an insertion site of the interosseous membrane or tendon. The FNP was present in the proximal third of the caudal surface of diaphysis. The narrowest area was just between the middle and distal third. The articular surface (*facies articularis carpea*) presented three well-circumscribed convex and smooth surfaces, two of which were part of the trochlea of the radius. Towards caudal, between the radial trochlea and the diaphysis, the transverse ridge was observed. In addition, a small medial styloid process (*processus styloideus medialis*) was observed. The grooves
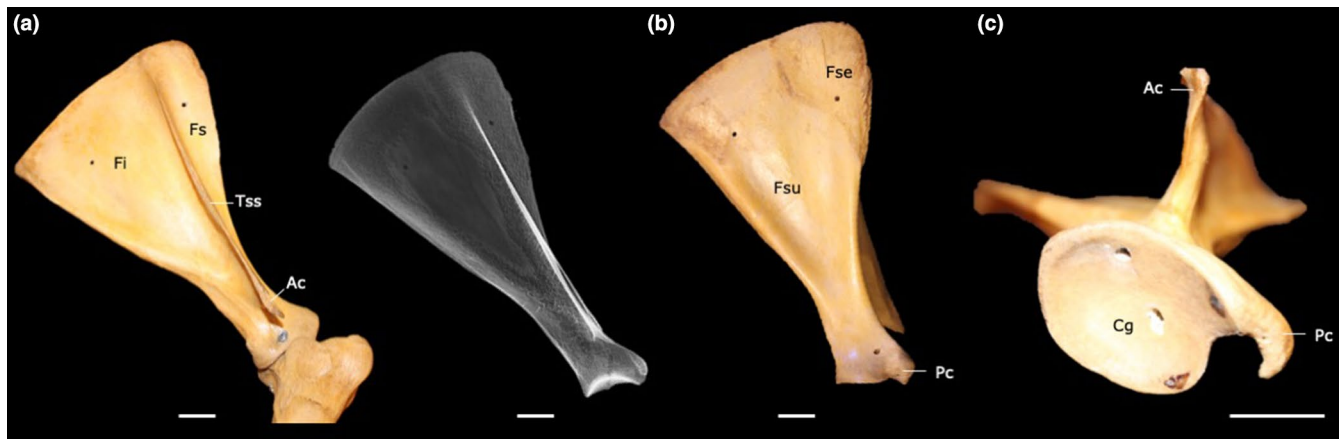
FIGURE 1 Scapula of Endangered Patagonian Huemul Deer. A, lateral and B, medial view. C, distal epiphysis. Fi, Fossa infraspinata; Fs, Fossa supraspinata; Tss, Tuber spinae scapulae; Ac, Acromion; Fse, Facies serrata cranial; Fsu, Fossa subscapularis; Pc, Processus coracoideus; Cg, Cavitas gleonoidalis. Bar: 20 mm
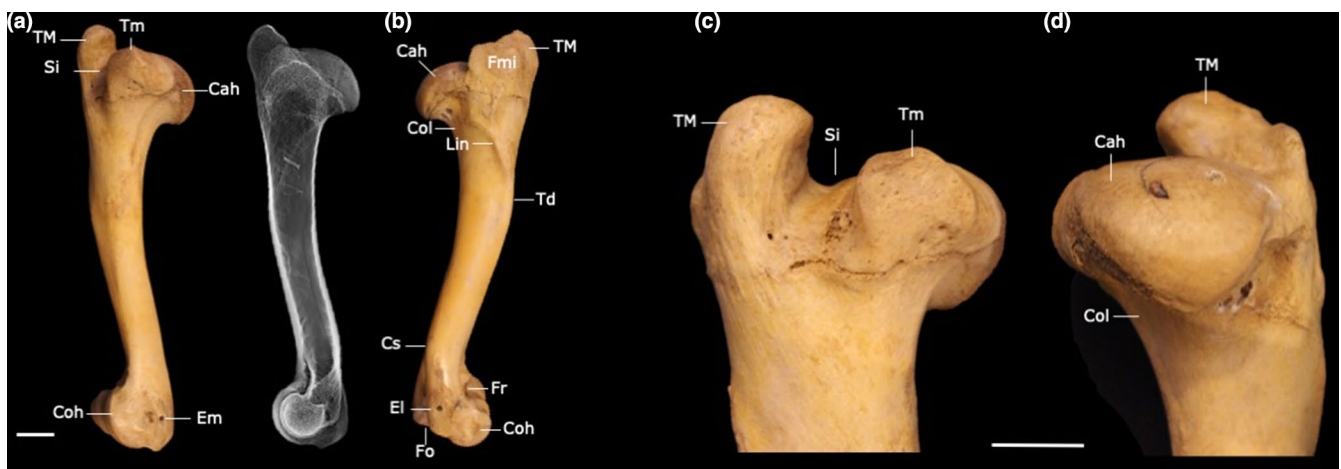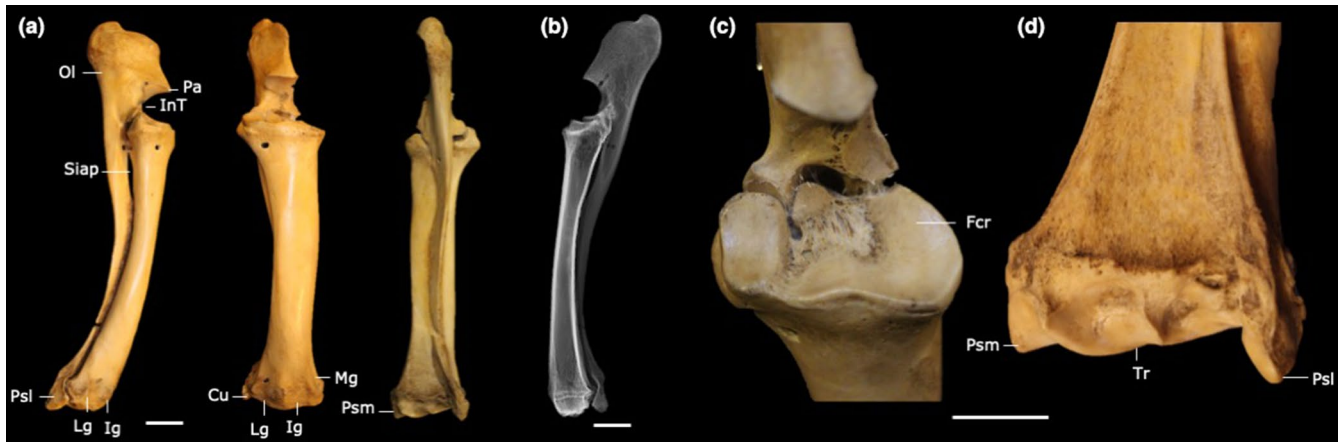

FIGURE 2 Humerus and radius of Endangered Patagonian Huemul Deer. A, medial and B, lateral view of humerus. C, cranial and D, caudal view of proximal epiphysis of humerus. TM, Tuberculum majus; Tm, Tuberculum minus; Si, Sulcus intertubercularis; Cah, Caput humeri; Em Epicondylus medialis; Coh, Condylus humeri; Fmi, Facies musculi infraspinati; Col, Collum humeri; Lin, Linea m. tricipital; Td, Tuberositas deoltoidea; Cs, Crista supracondylaris lateralis; El, Epicondylus lateralis; Fo, Fossa olecraniana; Fr, Fossa radialis Bar: 20 mm

(*sulcus tendini*) located on the cranial surface of the distal epiphysis of the radius were of particular attention: the medial sulcus was short and oblique, the intermediate sulcus was long and deep, and the lateral sulcus was the widest. Radio-ulna bones articulate at their extremities, leaving an interosseous space between their shafts. Radiopaque compact bone tissue was observed in the diaphysis, especially in the subchondral cortical plate of the radial trochlea. Also, trabecular bone tissue was observed distributed in the proximal and distal epiphysis.

The ulna (*ulna*) exceeded the length of the radius at both ends (Figure 3). The ulna was caudal to the radius in the proximal part of the antebrachium but lateral in the distal part. The olecranon was prominent, had a slightly concave and smooth medial surface, while the opposite surface was smooth and convex. The caudal margin was concave and projected distally to continue without precise limit with the caudal margin of the diaphysis. The cranial margin presented two portions limited by the processus anconeus: a smooth proximal

and a distal articular, represented by the trochlear notch. This structure was concave dorsoventrally and convex transversely—similar to a horse saddle—which articulated with the humeral condyle. The radial notch articulated the radius with the ulna. At the limit, between the two notches, the medial and lateral coronoid processes were located. The first was prominent and the second was smaller and less developed, both with the role of increase the articular surface between radius, ulna and humerus. The apex was the dorsal decussation of both margins and presented a protruding olecranon tuber (*tuber olecrani*). The diaphysis presented three surfaces: lateral, medial and cranial. The cranial surface was convex and rough, leaving a narrow antebrachial interosseous space. The FNP was located in the proximal third of this surface. The narrowest area was in the distal third. The head of the ulna presented a well-circumscribed articular circumference and a styloid process. It should be mentioned that ulna articulated with radius in two points: first, in the radial and trochlear notch, exactly in the centre of the caudal surface of the

FIGURE 3 Radius and ulna of Endangered Patagonian Huemul Deer. A and B, radio-ulna; C, proximal and D, distal epiphysis of radius; Ol, Olecranon; Pa, Processus anconeus; InT, Incisura trochlearis; Siap, Spatium interosseum antebrachii proximalis; Psl, Caput ulnae, processus styloideo lateralis; Lg, lateral groove; Ig, intermedium groove; Mg, medial groove; Psm, Processus styloideus medialis; Fcr, Fovea capitis radii; Tr, Trochlea radii. Bar: 20 mm
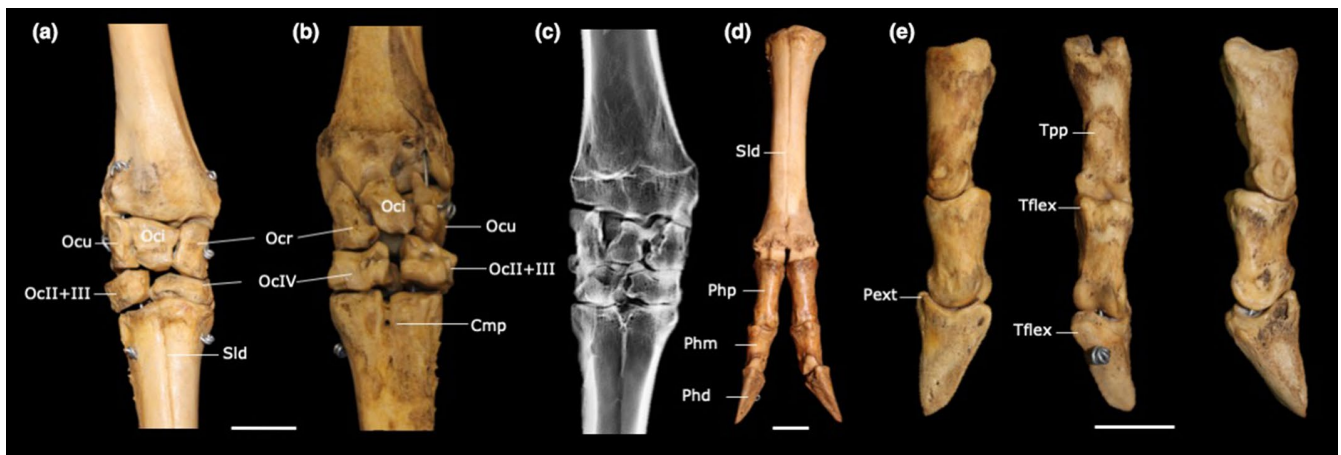
FIGURE 4 Bones of hand of Endangered Patagonian Huemul Deer. A, dorsal; B, palmar; C, palmaro-dorsal view; D, dorsal; E, acropodium. Ocu, Os carpi ulnare; Oci, Os carpi intermedium; Ocr, Os carpi radiale; OcII + III, Os carpale II et III; OcIV, Os carpale IV; Cmp, Canalis metacarpi proximalis; Sld, Sulcus longitudinalis dorsalis; Php, Phalanx proximalis; Phm, Phalanx media; Phd, Phalanx distale; Tpp, Trigonum phalangis proximalis; Tflex, tuberositas flexoria; Text, tuberositas extensoria. Bar: 20 mm

radius proximal epiphysis; and second, with the lateral portion of the distal epiphysis of the radius, in the articular circumference. Also, ulnar lateralisation towards distal was observed. The shaft of ulna presented a radiopaque proximal and distal portion (compact bone tissue) and a middle radiolucent portion (trabecular bone tissue).

In the skeleton of the hand (Figure 4; *autopodium*), the carpal bones were distributed in two rows: (a) an antebrachial row, represented by three bones: *os carpi ulnaris*, *os carpi intermedium* and *os carpi radiale*, and (b) a metacarpal row, represented by two bones: *os carpale IV* and *os carpale II et III*.

Metacarpal bones were represented by the fusion of metacarpals III and IV. The base is linked to the distal range of the carpal bones. Lateral on the articular face of the base a triangular surface was observed and was related to the carpal IV, towards the medial, a smooth and quadrilateral surface related to the carpal II + III was observed. In the diaphysis, the expression of the fusion is the

dorsal and palmar longitudinal grooves, flanked by the proximal and distal metacarpal canals (*canalis metacarpi proximalis et distalis),* which perforate the bone from dorsal to palmar. In addition, medial in the proximal epiphysis presented a prominent metacarpal III tuberosity (*tuberositas ossis metacarpi III*). The narrowest section of the diaphysis was between the proximal and middle third. The distal epiphysis presented two trochleae, whose axial lip was the lowest. Regarding the digits (*acropodium; ossa digitorum manus*), two were observed in each hand and both reached the ground. Each presented three phalanges (*phalanx proximalis, media et distalis*). The proximal phalanx (*phalanx proximalis*) presented a broad base, a well-defined body and apex, three faces and two margins. The base is the most prominent and had an asymmetrical articular face, which presented a surface of concavity pronounced dorsally. In the base and palmar face, two processes were observed, separated by a small fossa, were projected distally, by

the palmar face, in two converging ridges forming the triangle of the proximal phalanx (*trigonum phalangis proximalis)*. The axial face was flat, and the dorsolateral face was convex. The caput was less prominent, a trochlea with unequal lips was observed being the lateral lower than the medial. The middle phalanx (*phalanx medialis*) is complementary to the distal face of the proximal phalanx. On the palmar face, it presented a small relief that protruded towards the proximal and ended in the flexor tuberosity (*tuberositas flexoria*). In addition, in the dorsolateral face it presented an extensive process projected towards proximal. In the caput, a trochlea of two lips was observed, the lateral one was more prominent. The distal phalanx (*phalanx distale*) had a pyramidal shape, two faces, two margins and three angles. The solear face (in relation to the support plane) is rough, presented a weak semilunar line. The cutaneous plane was smooth towards the apex, and the flexor face was rough and robust, presenting a prominent flexor tubercle.

4 | DISCUSSIONS

The present study is the first description of the gross anatomy of the bones of thoracic limb (*ossa membri thoracici*) of the Patagonian huemul deer. We have described the osteology of the thoracic appendicular skeleton only in three specimens due to mainly its conservation status and particularly due to the scarce amount of living specimens available for biometric studies, the regulatory mechanisms and the difficult access to cadaverous material which makes it complex to obtain or manage it for scientific activity. Therefore, the presented morphological data are limited by sample size and by itself do not allow generalisations outside of the study area. The knowledge obtained in this study is valuable as a reference for clinical use, surgery, biomedical research and teaching, as well as relevant for the identification of species for interpretive purposes in field explorations. Slight variations among specimens were encountered when the features of the skeleton were assessed. These variations included size and appearance.

Regarding the thoracic limb skeleton, a triangular and prominent scapula, typical of ruminants, was observed. It was wide, with large cranial and caudal borders that allow an adequate insertion of scapular vertebral muscles, such as the omotransverse or rhomboid muscles, supporting body weight and giving stability to the shoulder joint (Getty & Sisson, 1975). A wide and deep glenoid cavity, the absence of clavicle and the acromion length similar to that observed in sheep (König & Liebich, 2005) suggest that the shoulder joint has reduced mobility, with limited movements, particularly extension–flexion and to a lesser extent abduction–adduction. On the other hand, the reduced size of the supraspinous fossa in relation to the infraspinous fossa draws the attention. This suggests differentiated roles of the supraspinous and infraspinous muscles with respect to the biomechanics and stability of the scapulohumeral joint, a type of collateral ligament (Kardong, 2013). This has been described in animals with the same osteological morphology, such as *Ozotoceros bezoarticus* (a South American deer) and *Axis axis* (an Asian deer) by

Vazquez (2015), who attributes an extensor role to the supraspinous muscle and abductor to the infraspinous muscle in the shoulder joint. Overall, the scapula presented similarities with what was described in *Ozotoceros bezoarticus* and *Axis axis*, especially for the muscular insertion lines that were observed between the serrata surfaces and the subscapular fossa. The abduction capacity of the shoulder joint is based on the presence of a prominent acromion (Kardong, 2013). In the case of the Patagonian huemul, the observed acromion was high but relatively short in length, not exceeding the scapular neck. This would decrease the abduction capacity of the deltoid muscle on the shoulder joint.

With respect to the humerus, the symmetry and medium-sized articular surface of the humeral head contrast with the size observed in other ruminants (Getty & Sisson, 1975). Compared with sheep, in the diaphysis the deltoid tuberosity is moderate in size, which suggests the presence of moderate tension loads in the deltoid muscle tendon. On the contrary, the teres minor tuberosity is prominent, broad and rough. The articular surface of the distal epiphysis is asymmetric, presenting a head and a trochlea, which provide an adequate relationship between articular surfaces for extension and flexion in the elbow joint. However, they diminish the freedom of movement of the ulna, limiting its supination. In addition, similar to ovine, a poorly developed lateral supracondylar crest was observed, which is the site of origin of the brachioradialis muscle, a supinator muscle of the forearm.

The radial notch of the ulna is deep, forming a well-circumscribed concavity with the proximal articular surface of the radius, which gives support to the elbow joint during the movements of extension and flexion. The epiphysis of the radius and the ulna articulate mainly in their more proximal regions. The ulna presented a narrow diaphysis, unlike the prominent diaphysis of the radius, which suggests that the biomechanical forces in the forearm are supported by the radius. According to the description of the thoracic limb muscles in other ruminants (Getty & Sisson, 1975; König & Liebich, 2005), such as sheep and goats, we hypothesised that powerful flexor muscles are present in the huemul thoracic limb due to the presence of a large teres major tuberosity (humerus) and the radial tuberosity (radius), both wide, rough and prominent. These provide insertion sites to the teres major muscle and brachial biceps, respectively. This characteristic suggests a natural and accentuated capacity of flexion of the shoulder and elbow described in large domestic animals (Nickel et al., 1986) and other vertebrates (Kardong, 2013). The latter could relate to the need to cushion the jumps that the deer perform. Nevertheless, among the studied skeletons, the depth of the radial fossa of the humerus observed in skeleton "A" contrasts with what was observed in "B" and "C," where it is not significantly deep. The former phenomenon has been evidenced in animals with morphological adaptations that help to flex the elbow joint (König & Liebich, 2005). Both the radius and the ulna presented a slightly straight body and particularly in the radius, a relative disto-medial obliquity is suggested, similar to that observed in other ungulates as a result of the regular use of the thoracic limb in an extended position (Nickel et al., 1986).

The morphological differences in the forearm skeleton between specimens studied we attribute it to the functional needs of the animal and to the direct influence of the habitat on the morphology of the appendicular skeleton, id est, the particularities of the habitat in which these animals lived could have influenced the morphological characteristics of the appendicular skeleton, especially in the thoracic limb, and perhaps each bones of the forearm skeleton demonstrate these differences in terms of functional needs (Flueck & Smith-Flueck, 2011; Oftadeh, Perez-Viloria, Villa-Camacho, Vaziri, & Nazarian, 2015). Regarding the carpal bones, in the three specimens studied, we found only five bones. However, in other cervids such as Axis axis or Ozotoceros bezoarticus, six bones have been described, including an accessory bone (Vazquez, 2015). Our background does not allow us to conclude (nor exclude) that there is an accessory bone in Huemul deer. The metacarpal bone demonstrates the characteristic bone fusion presented by the majority of ungulates, typical in sheep and cattle (König & Liebich, 2005). Regarding the phalanges, the presence of a prominent flexor tuberosity of the middle and distal phalanx, site of tendon insertion, suggests the existence of powerful flexor tendons of the palmar region of the hand.

In conclusion, it was possible to describe in detail the thoracic limb bones of the Patagonian Huemul Deer in morphometric, anatomical and radiographic terms. We observe that it has bone characteristics more similar to small ruminants, such as sheep and goats, than to large ruminants. Also, the bones and bony eminences present in the thoracic limb suggest the presence of powerful flexor muscles in the scapulohumeral and elbow joints, useful to cushion the jumps. Also, the FNP differs in position with respect to domestic ungulates, which may be important to consider during surgical procedures. Finally, the radiographic data can provide new information about the tissue loading conditions in Patagonian huemul, so that this new knowledge can be of great importance for a better understanding of mechanically induced or adaptive changes in bone produced by habitat or other ecological-evolutionary phenomena.

ACKNOWLEDGEMENTS

CONFLICT OF INTEREST

The authors declare no conflicts of interest.

ORCID

Paulo Salinas https://orcid.org/0000-0003-2273-0904
Samuel Núñez-Cook https://orcid.org/0000-0003-3778-6812
Abigail Arenas-Caro https://orcid.org/0000-0002-1268-8733

REFERENCES

Black-Decima, P. A., Corti, P., Díaz, N., Fernandez, R., Geist, V., Gill, R., … Wittmer, H. (2016) *Hippocamelus bisulcus. The IUCN Red List of Threatened Species 2016*. Retrieved from https://www.iucnredlist.org/species/10054/22158895 Accesed 17 July 2019.

Corti, P., Saucedo, C., & Herrera, P. (2013). Evidence of bovine viral diarrhea, but absence of infectious bovine rhinotracheitis and bovine brucellosis in the endangered huemul deer (*Hippocamelus bisulcus*) in Chilean Patagonia. *Journal of Wildlife Diseases*, 49, 744–746.

Flueck, W. T. (2015). Osteopathology and selenium deficiency co-occurring in a population of endangered Patagonian huemul (*Hippocamelus bisulcus*). *BMC Research Notes*, 8, 330. https://doi.org/10.1186/s13104-015-1291-9

Flueck, W. T., & Smith-Flueck, J. M. (2011). Osteological comparisons of appendicular skeletons: A case study on Patagonian huemul deer and its implications for conservation. *Animal Production Science*, 51, 327–339. https://doi.org/10.1071/AN10174

Flueck, W. T., & Smith-Flueck, J. M. (2017). Troubling disease syndrome in endangered live Patagonian huemul deer (*Hippocamelus bisulcus*) from the Protected Park Shoonem: Unusually high prevalence of osteopathology. *BMC Research Notes*, 10, 739. https://doi.org/10.1186/s13104-017-3052-4

Getty, R., & Sisson, S. (1975). *Sisson and Grossman's the Anatomy of the Domestic Animals*, 5th ed. Philadelphia, USA: W.B. Saunders Company.

González-Acuña, D., Saucedo, G. C., Corti, P., Casanueva, M. E., & Ciccino, A. (2009). First records of the louse *Solenopotes binipilosus* (Insecta: Phthiraptera) and the mite *Psoroptes ovis* (Arachnida: Acari) from wild southern huemul (*Hippocamelus bisulcus*). *Journal of Wildlife Diseases*, 45, 1235–1238. https://doi.org/10.7589/0090-3558-45.4.1235

International Committee on Veterinary Gross Anatomical Nomenclature (ICVGAN) (2017). *Nomina Anatomica Veterinaria*. 6th ed. Ghent (Belgium), Columbia, MO (U.S.A.), Rio de Janeiro (Brazil): Editorial Committee Hanover (Germany).

Iriarte, A., Donoso, D. S., Segura, B., & Tirado, M. (2017). *El Huemul de Aysén y otros rincones*. 1st ed. Aysén, Chile: Ediciones Secretaría Regional Ministerial de Agricultura de la Región de Aysén y Flora & Fauna Chile Limitada.

Kardong, K. V. (2013). *Vertebrates: Comparative Anatomy, Function, Evolution*, 7th ed. Boston, USA: McGraw-Hill Higer Education.

König, H., & Liebich, H. (2005). *Anatomía de los Animales Domésticos*, Tomo 1 (2nd ed.). Madrid, España: Médica Panamericana.

Morales, N., Aldridge, D., Bahamonde, A., Cerda, J., Araya, C., Muñoz, R., … Retamal, P. (2017). Corynebacterium pseudotuberculosis infection in Patagonian Huemul (*Hippocamelus bisulcus*). *Journal of Wildlife Diseases*, 53, 621–624. https://doi.org/10.7589/2016-09-213

Nickel, R., Schummer, A., Seiferle, E., Wilkens, H., Wille, K. H., & Frewein, J. (1986). *The anatomy of the domestic animals. (vol. 1) The Locomotor System of the Domestic Mammals*, 5th ed. Berlin: Springer-Verlag.

Oftadeh, R., Perez-Viloria, M., Villa-Camacho, J. C., Vaziri, A., & Nazarian, A. (2015). Biomechanics and mechanobiology of trabecular bone: A review. *Journal of Biomechanical Engineering*, 137(1), 0108021–01080215. https://doi.org/10.1115/1.4029176

Salgado, M., Corti, P., Verdugo, C., Tomckowiack, C., Moreira, R., Durán, K., … Tejeda, C. (2017). Evidence of Mycobacterium avium subsp. paratuberculosis (MAP) infection in huemul deer (*Hippocamelus bisulcus*) in patagonian fjords. *Austral Journal of Veterinary Sciences*, 49, 135–137. https://doi.org/10.4067/S0719-81322017000200135

Vazquez, N. S. (2015). *Anatomía de los miembros torácico y pelviano del venado de campo (Ozotoceros bezoarticus) y del ciervo axis (Axis axis)*. Tesis de grado. Universidad de la República (Uruguay). Facultad de Veterinaria. Retrieved from https://www.colibri.udelar.edu.uy/jspui/handle/20.500.12008/10300.

Vélez-García, J. F., Monroy-Cendales, M. J., & Castañeda-Herrera, F. E. (2018). Morphometric, anatomic and radiographic study of the

scapula in the white-footed tamarin (*Saguinus leucopus*): Report of scapular cartilage and one variation in cranial (superior) transverse scapular ligament. *Journal of Anatomy, 234*, 120–131. https://doi.org/10.1111/joa.12899

Vila, A. R., Briceño, C., Mc Aloose, D., Seimon, T. A., Armién, A. G., Mauldin, E. A., … Uhart, M. M. (2019). Putative parapoxvirus-associated foot disease in the endangered huemul deer (*Hippocamelus bisulcus*) in Bernardo O'Higgins National Park. *Chile. Plos ONE, 14*(4), e0213667. https://doi.org/10.1371/journal.pone.0213667

Vila, A. R., López, R., Pastore, H., & Serret, A. (2006). Current distribution and conservation of the huemul (*Hippocamelus bisulcus*) in Argentina and Chile. *Mastozoología Neotropical, 13*, 263–269.